Available online at www.sciencedirect.com
ScienceDirect
BioSystems 89 (2007) 287–293
BioSystems
www.elsevier.com/locate/biosystems

Effect of stimulus-driven pruning on the detection of spatiotemporal patterns of activity in large neural networks

Javier Iglesias[a,b]*, Alessandro E.P. Villa[a,b,1]

[a] *Inserm, U318, Laboratoire de Neurobiophysique, Université Joseph Fourier, Grenoble 1, CHU Michallon Pavillon B, BP 217, F-38043 Grenoble Cedex, France*

[b] *Neuroheuristic Research Group, Information Systems Institute, ISI, Internef, University of Lausanne, CH-1015 Lausanne, Switzerland*

Received 21 December 2005; accepted 26 May 2006

Abstract

Adult patterns of neuronal connectivity develop from a transient embryonic template characterized by exuberant projections to both appropriate and inappropriate target regions in a process known as *synaptic pruning*. Trigger signals able to induce synaptic pruning could be related to dynamic functions that depend on the timing of action potentials. We stimulated locally connected random networks of spiking neurons and observed the effect of a spike-timing-dependent synaptic plasticity (STDP)-driven pruning process on the emergence of cell assemblies. The spike trains of the simulated excitatory neurons were recorded. We searched for spatiotemporal firing patterns as potential markers of the build-up of functionally organized recurrent activity associated with spatially organized connectivity.

Keywords: Preferred firing sequence; Locally connected random network; Spike-timing-dependent synaptic plasticity; Spiking neural network

1. Introduction

There is experimental evidence that the cerebral cortex develops as a whole rather than regionally, as synaptogenesis proceeds concurrently in all cortical areas and layers. Simultaneous overproduction of a critical mass of synapses in each cortical area may be essential for their parallel emergence through competitive interactions between extrinsic afferent projections. Such competition has been observed between the projections of the two eyes during the formation of visual centers (Hubel et al., 1977; Rakic, 1981).

Genetic programs are assumed to drive the primordial pattern of neuronal connectivity through the actions of a limited set of trophic factors and guidance cues, initially forming excessive axonal and dendritic branches and synapses, distributed somewhat diffusely (Innocenti, 1995). Then, refinement processes act to correct initial inaccuracies by pruning inappropriate connections while preserving appropriate ones. The embryonic nervous system is refined over the course of development as a result of the twin processes of cell death and selective axon pruning. It is generally agreed that changes in cortical function are associated with corresponding alterations in the density and arrangement of synaptic circuits. The density of synapses continues to increase during infancy and remains above

* Corresponding author at: Neuroheuristic Research Group, Information Systems Institute, ISI, Internef, University of Lausanne, CH-1015 Lausanne, Switzerland. Tel.: +41 21 692 35 87; fax: +41 21 692 35 85.
[1] Tel.: +33 4 76 76 56 25; fax: +33 4 76 76 56 19.
E-mail addresses: Javier.Iglesias@unil.ch (Javier Iglesias), Alessandro.Villa@ujf-grenoble.fr (Alessandro E.P. Villa).
URL: http://www.neuroheuristic.org.

0303-2647/$ – see front matter © 2006 Elsevier Ireland Ltd. All rights reserved.
doi:10.1016/j.biosystems.2006.05.020

adult levels. After a relatively short period of stable synaptic density, a pruning process begins: synapses are constantly removed, yielding a marked decrease in synaptic density. This process continues until puberty, when synaptic density stabilizes at adult levels which are maintained until old age (Huttenlocher, 1979). It was observed through widespread brain regions including cortical areas (Bourgeois and Rakic, 1993; Huttenlocher et al., 1982) and the projection fibers between hemispheres (Innocenti, 1995). Pruning may also play a role in establishing topographic maps, as it can be seen in the retinotectal system (Nakamura and O'Leary, 1989). The relation between synaptic efficacy and synaptic pruning (Chechik et al., 1999; Mimura et al., 2003) suggests that the weak synapses may be modified and removed through competitive "learning" rules. Trigger signals able to induce synaptic pruning could be related to dynamic functions that depend on the timing of action potentials.

In this article, we studied the emergence of cell assemblies out of a locally connected random network of integrate-and-fire units distributed on a 2D lattice (Iglesias et al., 2005) stimulated in both temporal and spatial dimensions. The originality of our study stands on the size of the network, 10,000 U, the duration of the experiment, 10^6 time steps (1 time step = 1 ms), and the application of spike-timing-dependent synaptic plasticity (STDP) rule that is a change in the synaptic strength based on the ordering of pre- and post-synaptic spikes (Bell et al., 1997). Among several STDP rules (Roberts and Bell, 2002) we selected a rather simple one compatible with a custom designed hardware implementation (Eriksson et al., 2003; Torres et al., 2004). This hardware is the core of electronic devices, called POEtic, whose architecture include features derived from some of the properties present in living beings, like evolution, development, self-repair, self-replication and learning (Tyrrell et al., 2003). The combination of partial and total dynamic reconfiguration, as well as the self-configuration and dynamic routing capabilities make these devices an ideal candidate for the efficient implementation of large-scale spiking neural network models. In our study the synaptic modification rule was applied only to the excitatory–excitatory (exc, exc) connections. STDP is expected to strengthen the connections among neurons that belong to cell assemblies characterized by recurrent patterns of firing. Conversely, those connections that are not recurrently activated might decrease in efficiency and eventually be eliminated. The main goal of our study is to determine whether or not, and under which conditions, such cell assemblies may emerge from a large neural network receiving background noise and content-related input organized in both temporal and spatial dimensions.

2. Models and methods

2.1. Simulation protocol

The complete neural network model is described in details in Iglesias et al. (2005). Some aspects that were not discussed in that reference are presented here, along with a sketch description of the model. Integrate-and-fire units (80% excitatory and 20% inhibitory) were laid down on a squared 2D lattice according to a space-filling quasi-random Sobol distribution. Networks of size 100 × 100 U were simulated. Sparse connections between the two populations of units were randomly generated according to a two-dimensional Gaussian density function such that excitatory projections were dense in a local neighborhood, but low probability long-range excitatory projections were allowed. Edge effects induced by the borders were limited by folding the network as a torus (Iglesias et al., 2005). All units of the network were simulated by leaky integrate-and-fire neuromimes. The state of the ith unit $S_i(t)$ was a function of the membrane potential and a threshold, taking the value $S_i(t) = 1$ when the unit was spiking, and $S_i(t) = 0$ when it was not spiking. After a spike, the membrane potential was reset, and the unit entered an absolute refractory period set to 3 ms for excitatory units, and 2 ms for inhibitory units. Each unit received a background activity that followed an independent and uncorrelated Poisson process of mean $\lambda = 5$ spikes/s.

Before the simulation started, two distinct sets of 400 excitatory units were randomly selected from the 8000 excitatory units of the network, labeled sets A and B. Each set was divided into 10 ordered groups of 40 U, $A = \{A_1, A_2, \ldots, A_{10}\}$ and $B = \{B_1, B_2, \ldots, B_{10}\}$. At each time step during a stimulus presentation, the 40 U of one group received a large excitatory input on their membrane, leading to their synchronous firing. The 10 groups of a set were stimulated following an ordered sequence, thus defining a reproducible spatiotemporal stimulus composed by the repetition of sequences lasting 10 ms each (Fig. 1). Then, one stimulus presentation lasted 100 ms. The following protocols were used: (Pr1) no stimulus; (Pr2) 10× sequence A; (Pr3) 10× sequence B; (Pr4) 5× sequence A followed by 5× sequence B; (Pr5) 5× sequence B followed by 5× sequence A; (Pr6) a random, equiprobable mix of protocols 4 and 5.

2.2. Spike-timing-dependent plasticity rule

It is assumed *a priori* that a modifiable synapse between pre-synaptic unit j and post-synaptic unit i is characterized by discrete activation levels $A_{ji}(t)$, according to recent biological evidence (Montgomery and Madison, 2004). In the current study we attributed a fixed activation level (meaning no synaptic modification) $A_{ji}(t) = 1$, to (exc, inh), (inh, exc), and (inh, inh) synapses while activation levels were allowed to take

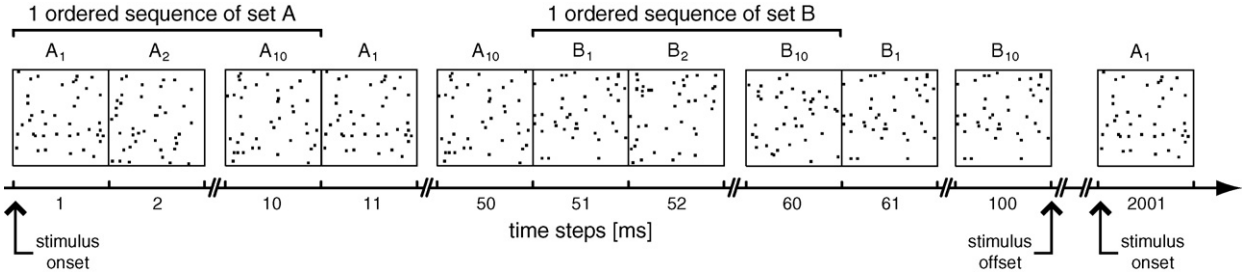

Fig. 1. Example of one *AB* (Pr4) stimulus presentation lasting 100 ms. At each time step, dots mark the group of 40 U receiving a large excitatory input on their membrane.

one of $A_{ji}(t) = \{0, 1, 2, 4\}$ for (exc, exc) synapses, $A_{ji}(t) = 0$ meaning that the synapse became permanently dead.

A real-valued variable $L_{ji}(t)$ was used to implement the spike-timing-dependent plasticity rule (STDP) for $A_{ji}(t)$, with integration of the timing of the pre- and post-synaptic activities. On the generation of a post-synaptic spike (i.e., when $S_i(t) = 1$), the value L_{ji} was incremented as a function of the interval determined by the previous pre-synaptic spike at that synapse (Fig. 2). Conversely, L_{ji} was decreased as a function of the timing of the previous post-synaptic spike (i.e., when $S_j = 1$). This rule is summarized by the following equation:

$$L_{ji}(t+1) = L_{ji}(t) + (S_i(t)M_j(t)) - (S_j(t)M_i(t))$$

where $S_i(t)$, $S_j(t)$ are the state variables of the ith and j units and $M_i(t)$, $M_j(t)$ are interspike decay functions. $M_i(t)$ may be viewed as a "memory" of the last interspike interval characterized by a plasticity time constant. The variable $L_{ji}(t)$ was a user-defined boundary of attraction $L_0 < L_1 < L_2 < \cdots < L_{N-1} < L_N$ satisfying $L_{k-1} < [A_k] < L_k$ for $k = 1, \ldots, N$. This means that whenever $L_{ji} > L_k$ the activation variable A_{ji} jumped from state $[A_k]$ to $[A_{k+1}]$. Conversely, A_{ji} jumped from state $[A_{k+1}]$ to $[A_k]$ if $L_{ji} < L_k$. After a jump L_{ij} was reset to $L_{ij}(t+1) = (L_k + L_{k+1})/2$ (Iglesias et al., 2005).

2.3. Spike train analysis

Spatiotemporal firing patterns (often referred to as "preferred firing sequences") are defined as sequences of intervals with high temporal precision (of the order of few milliseconds) between at least three spikes (triplet) that recur at levels above those expected by chance (Villa, 2000). The pattern detection algorithm begins with finding all single or multi-neuron sequences of intervals that repeat two or more times within a record. Secondly, the "pattern grouping algorithm" (Tetko and Villa, 2001) computed how many of such sequences of intervals can be expected by chance, clusterizes into one group those sequences of intervals with slight difference in spike timing, and provides confidence limits for this estimation (Fig. 3). The general notation describes the timing features of a triplet as follows: $\langle a,\ b,\ c; t_1 \pm \Delta t_1,\ t_2 \pm \Delta t_2 \rangle$. This means that the pattern starts with a spike of unit #a, then $t_1 \pm \Delta t_1$ ms later a spike of unit #b and a third spike of unit #c $t_2 \pm \Delta t_2$ ms from pattern start.

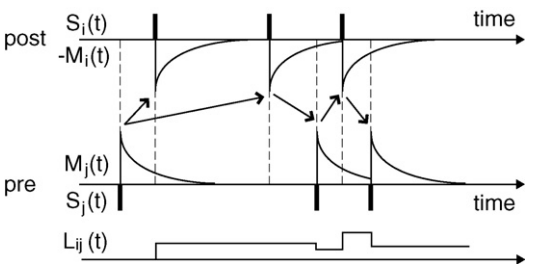

Fig. 2. Graphical representation of the variables $S(t)$, $M(t)$ and $L(t)$ in the STDP rule. Bold ticks mark the occurrences of spikes ($S(t) = 1$) that correspond to the times when $M(t)$ is reset.

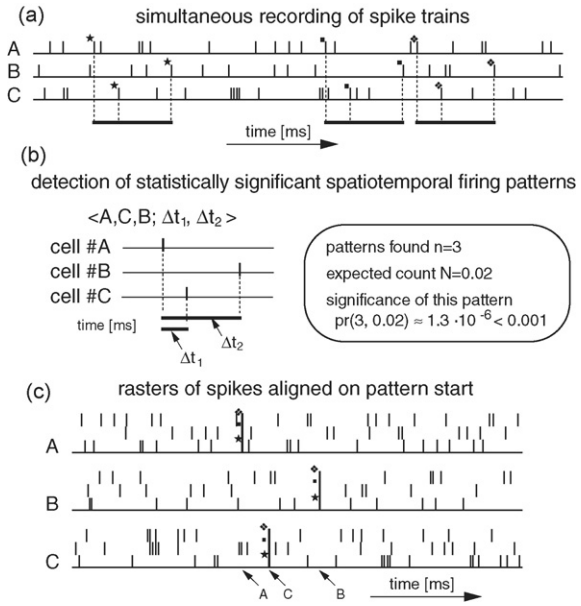

Fig. 3. Outline of the general procedure followed by pattern detection algorithms: (a) analysis of a set of simultaneously recorded spike trains. Three cells, labeled A–C, participate to a patterned activity. Three occurrences of a precise pattern are detected. Each occurrence of the pattern has been labeled by a specific marker in order to help the reader to identify the corresponding spikes; (b) estimation of the statistical significance of the detected pattern; (c) display of pattern occurrences as a raster plot aligned on the pattern start.

The initial 200 s of simulation were not recorded because the synaptic pruning is very active and the network is not in a steady state. At time 500 s the simulation was stopped and the topology of the network was analyzed. Then, the simulation continued until $t = 1000$ s either with STDP-driven pruning maintained as before *continuous pruning* – or without synaptic pruning (i.e., pruning ended after the first 500 s) – *interrupted pruning*. This means that we recorded the spike trains in the interval [200–500 s], then in the intervals [500–1000 s] of either pruning condition. The interval [450–500 s] is assumed to be representative of a "mature" level of pruning reached by the network. Notice that in this interval the stimulus was presented 25 times (once every 2000 ms). The stimulus triggered transient changes in firing rate during the first part of the inter-stimulus interval, i.e., up to 1000 ms after its onset. Such transient activity could affect the efficiency of the pattern grouping algorithm Tetko and Villa (1997). Thus, for the present study, we used only the recordings during the second part of the inter-stimulus interval as *searchable spike train* for the spatiotemporal firing patterns. The algorithm was set to find patterns of at least three spikes (triplets), with a minimal significance level of 5%, repeating at least seven times provided the entire pattern lasted not more than 200 ms and was repeated with a jitter $\Delta t_i = \pm 3$ ms at most.

The autorenewal densities were computed, according to Abeles (1982), for all units that participated to preferred firing sequences. Whenever more than 1 U was found in a preferred firing sequence we computed also all pairwise cross-correlograms. Such auto- and cross-correlograms are referred to as 'regular' correlograms. We computed the 'shift predictor' (Perkel et al., 1967) in order to estimate the effect of the stimuli on the firing rate modulations, by shifting the trials, triggered on stimulus onset, with respect to each other in wrap-around fashion. The net effect of cell assembly interactions was obtained by the 'differential' correlogram, which is the difference between regular and shift predictor correlograms.

3. Results

3.1. Stimulus-dependent projections

Each simulation run lasted 10^6 discrete time steps (1 ms per time step), corresponding to a duration of about 16 min. After a stabilization period of 1000 ms without any external input, the stimulus (lasting 100 ms, see Section 2) was presented once every 2000 ms. Along one simulation run the network received overall 500 stimulus presentations.

For each distinct initial condition, we searched among the pool of 8000 excitatory units those that were characterized by stimulus-dependent projections, that means all units that (a) were not directly stimulated; (b) had no input or output (exc, exc) connections in absence of stimulus (protocol Pr1); (c) but maintained strong input and output (exc, exc) connections for any stimulation protocol; (d) had a mean discharge rate less than 40 spikes/s to avoid a filtering bias due to spatiotemporal firing pattern analysis (Tetko and Villa, 1997). Each simulation run was analyzed at time $t = 500$ s and the units that complied with the above criteria formed a cell group labeled *stimulus-dependent assembly*. This analysis was carried out for each seed and stimulation protocol combination. The stimulus-dependent cell assemblies included 4–54 U.

3.2. Spatiotemporal firing patterns

Spatiotemporal firing patterns of complexity 3 (triplets) and 4 (quadruplets) were searched in the interval [450–500 s] in either protocol. An overall amount of 44 triplets and 82 quadruplets were significantly detected by the pattern grouping algorithm (Tetko and Villa, 2001). Most (97/126) of the significant firing patterns of either complexity 3 or 4 were composed by repetitions of spikes by 1 U (e.g., we found 22 occurrences of the triplet $\langle 6, 6, 6; 131 \pm 2, 183 \pm 3\rangle$ with protocol Pr4). Two cases of quadruplets are presented in detail to illustrate several characteristics of interest.

3.2.1. Case 1

The pattern $\langle 1, 2, 3, 4; 2 \pm 0.5, 30 \pm 1.5, 62 \pm 1.5\rangle$ was composed by spikes generated by four distinct units during protocol Pr5 (in this protocol the stimulus sequence *B* repeated five times followed by five repetitions of sequence *A*). This pattern (Fig. 4) was observed five times in the interval [450–500 s], and its statistical significance was 1.5×10^{-2} (Tetko and Villa, 2001). In this example it is interesting to notice that the delay between the first two events of the pattern was only 2 ms. This short delay might suggest that a tendency to synchronous firing between units #1 and #2 could favor the detection of the pattern. In fact the correlation between the pair of units (#1, #2) did not show any peak centered near time zero, i.e., no signs of significant synchronous firing of these units. Further analysis of the timings of the spatiotemporal pattern with respect to the stimulation onset did not show any time-locked correlation between stimulus and pattern occurrence. The analysis with respect to pruning dynamics (Fig. 4d) suggested that the interruption of pruning maintained somewhat the occurrence of the pattern up to ca. $t = 750$. After this time the pattern appeared at random times and was not significant. In the case of continuous pruning the pattern tended to appear at random times much earlier, from $t = 600$ s onward.

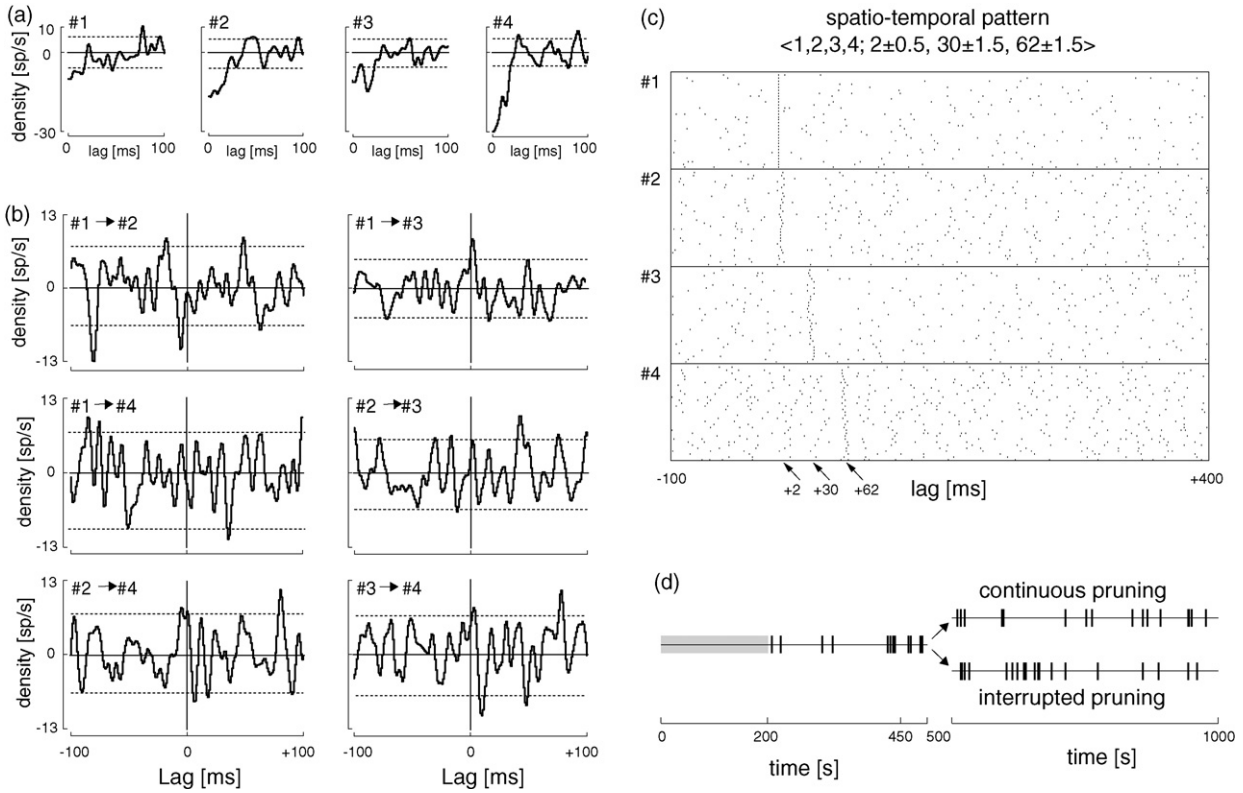

Fig. 4. Case 1: spatiotemporal firing pattern $\langle 1, 2, 3, 4; 2 \pm 0.5, 30 \pm 1.5, 62 \pm 1.5\rangle$ formed by spikes recorded from four units: (a) differential auto-correlograms and (b) differential cross-correlograms of the four units smoothed by Gaussian shaped bin of 5 ms width. The dotted lines represent 99% confidence limits calculated according to Abeles (1982). The average firing rates were 12.5, 18.6, 15.8, 30.3 spikes/s for units #1–4, respectively; (c) raster plot showing 33 repetitions of the pattern in the *continuous pruning* condition aligned on pattern start; (d) pattern occurrence timing plot: each vertical tick represents the start event of a pattern occurrence. Compare with Fig. 5d.

3.2.2. Case 2

The pattern $\langle 5, 5, 5, 5; 27 \pm 3, 99 \pm 3, 127 \pm 3\rangle$ was composed by spikes produced by one single unit, labeled here #5 (Fig. 5d). Between $t = 450$ and 500 during protocol Pr4 (in this protocol 5× sequence *A* were followed by 5× sequence it B) 15 repetitions of the pattern were observed. The statistical significance of this pattern of activity was 5×10^{-7}. No correlation could be found between the timings of the spatiotemporal pattern and the stimulation onset.

Fig. 5d shows how this pattern is affected by the pruning process. In the interval [200–500 s], the pattern was detected 62 times. After the pruning was stopped, at $t = 500$ s, the pattern appeared 118 times between $t = 500$ and 1000 and its rate of occurrence remained stable throughout this interval. In contrast, in the continuous pruning condition, the occurrences of the pattern tended to decrease. In this condition 20 repetitions of the pattern were observed in the interval [500–650 s], which is a significant rate, but only 19 repetitions were observed between $t = 650$ and 1000. The disappearance of this pattern is necessarily related to the pruning process, as it is the only difference between the two conditions. This suggests that after $t = 500$ s, the maintenance of the pruning process removed those connections that were somehow mandatory for the occurrence of the spatiotemporal pattern.

4. Discussion

This paper has presented some hints about the emergence of spatially organized cell assemblies embedded in a large neuronal network. The analysis of the spatial locations of the units whose activity participated to the preferred firing sequences did not reveal any characteristic distance or radius of the cell assemblies. Our results are obtained from a large simulated network but its size is very small compared to realistic brain circuits. We cannot discard, and in fact we suggest it, that "spatial clusters" might appear in simulations that involve network sizes one to two orders of magnitude larger than ours.

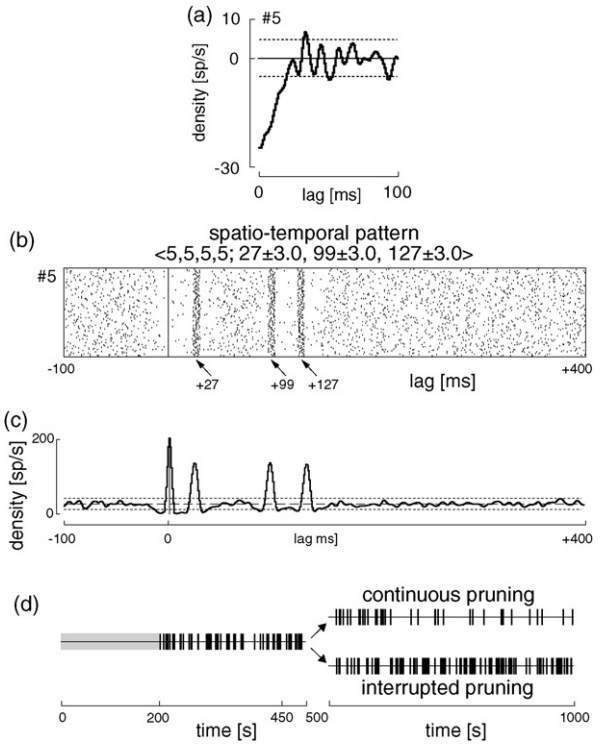

Fig. 5. Case 2: spatiotemporal firing pattern $\langle 5, 5, 5, 5; 27 \pm 3, 99 \pm 3, 127 \pm 3\rangle$ formed by spikes recorded from one same unit. The average firing rate was 16.5 spikes/s: (a) differential auto-correlogram smoothed by Gaussian shaped bin of 5 ms; (b) raster plot showing 180 epetitions of this pattern in the *interrupted pruning* condition aligned on pattern start; (c) spike density histogram of the raster *b* smoothed by Gaussian shaped bin of 5 ms; (d) pattern occurrence timing plot: each vertical tick represents the start event of a pattern occurrence. Compare with Fig. 4d.

We had previously observed that the unsupervised pruning process, associated with short and stable stimulation patterns, tended to organize units in strongly interconnected feed-forward assemblies (Iglesias et al., 2005). Synfire chains (Abeles, 1991) are layered diverging/converging chains of neurons discharging synchronously to sustain the propagation of the information through a feed-forward neural network. In the simulated activity presented here we found evidence of a significant excess of recurrent spatiotemporal firing patterns, thus suggesting an association between the emergence of layered topologies and the appearance of preferred firing sequences. The finding that such firing patterns were observed more frequently after the stabilization of the dynamics of the changes in synaptic strengths and after the pruning process was stopped suggests that optimal levels of pruning are necessary to let emerge those topologies able to sustain the recurrent activity that generates the preferred firing sequences. The stop or the reduction of pruning at some "mature" phase of the simulation might open the way to study developmental transitions somewhat comparable to those represented by childhood to adolescence and from adolescence to adulthood. Future simulations could be used to investigate models of metaplasticity (Abraham and Bear, 1996) and the association between the pruning phase and its capacity to induce recallable long-term memories.

The self-organization of spiking neurons into neuronal groups was also described in a study featuring large simulated networks connected through STDP including axonal conduction delays (Izhikevich et al., 2004). The main difference with our results is that Izhikevich et al. (2004) found disjoint small groups of interconnected neurons that exhibited correlated temporal patterns of activity not related to the emergence of layered structures. These differences might be due to the lack of axonal delays in our model and our implementation of the STDP rule based on state synapses (Montgomery and Madison, 2004) rather than by adjusting their efficacy along a continuum. An alternative view to explain the recurrence of preferred firing sequences is that the cell assembly topology does not necessarily correspond to feed-forward layers, but it could follow a "chaotic graph" topology. We intend a graph whose dynamic activity is deterministic in the "mature" state of the network and falling into dynamical attractors given initial patterns of activity. This alternative view is supported by the observation, in this study, of a majority (97/126) of spatiotemporal firing patterns formed by 1 U, i.e., patterns like $\langle a, a, a; t_1, t_2\rangle$. Additional theoretical arguments in favor of this interpretation are discussed in Villa (2000). Future studies of the simulate spike train dynamics will include calculation of correlation dimension and Lyapunov exponents. These new results might reveal further analogies with experimental data that demonstrated low dimensional chaotic attractors in the rat brain (Celletti et al., 1999; Celletti and Villa, 1996).

References

Abeles, M., 1982. Quantification, smoothing, and confidence limits for single-units' histograms. J. Neurosci. Meth. 5, 317–325.

Abeles, M., 1991. Corticonics: Neural Circuits of the Cerebral Cortex, 1st ed. Cambridge University Press.

Abraham, W.C., Bear, M.F., 1996. Metaplasticity: the plasticity of synaptic plasticity. Trends Neurosci. 19 (4), 126–30.

Bell, C.C., Han, V.Z., Sugawara, Y., Grant, K., 1997. Synaptic plasticity in a cerebellum-like structure depends on temporal order. Nature 387 (6630), 278–281.

Bourgeois, J., Rakic, P., 1993. Changes of synaptic density in the primary visual cortex of the macaque monkey from fetal to adult stage. J. Neurosci. 13, 2801–20.

Celletti, A., Froeschlé, C., Tetko, I.V., Villa, A.E.P., 1999. Deterministic behaviour of short time series. Meccanica 34, 145–152.

Celletti, A., Villa, A.E.P., 1996. Determination of chaotic attractors in the rat brain. J. Stat. Phys. 84, 1379–1385.

Chechik, G., Meilijson, I., Ruppin, E., 1999. Neuronal regulation: a mechanism for synaptic pruning during brain maturation. Neural Comput. 11, 2061–2080.

Eriksson, J., Torres, O., Mitchell, A., Tucker, G., Lindsay, K., 2003. Spiking neural network for reconfigurable POEtic tissue. Lect. Notes Comput. Sci. 2606, 165–173.

Hubel, D.H., Wiesel, T.N., LeVay, S., 1977. Plasticity of ocular dominance columns in monkey striate cortex. Philos. Trans. R. Soc. Lond. B: Biol. Sci. 278 (961), 377–409.

Huttenlocher, P.R., 1979. Synaptic density in human frontal cortex—developmental changes and effects of aging. Brain Res. 163 (2), 195–205.

Huttenlocher, P.R., de Courten, C., Garey, L.J., Van der Loos, H., 1982. Synaptogenesis in human visual cortex—evidence for synapse elimination during normal development. Neurosci. Lett. 33 (3), 247–252.

Iglesias, J., Eriksson, J., Grize, F., Tomassini, M., Villa, A.E., 2005. Dynamics of pruning in simulated large-scale spiking neural networks. BioSystems 79 (1), 11–20.

Iglesias, J., Eriksson, J., Pardo, B., Tomassini, M., Villa, A.E., 2005. Emergence of oriented cell assemblies associated with spike-timing-dependent plasticity. Lect. Notes Comput. Sci. 3696, 127–32.

Innocenti, G.M., 1995. Exuberant development of connections, and its possible permissive role in cortical evolution. Trends Neurosci. 18 (9), 397–402.

Izhikevich, E.M., Gally, J.A., Edelman, G.M., 2004. Spike-timing dynamics of neuronal groups. Cereb. Cortex 14, 933–44.

Mimura, K., Kimoto, T., Okada, M., 2003. Synapse efficiency diverge due to synaptic pruning following over-growth. Phys. Rev. E: Stat. Nonlin. Soft Matter Phys. 68, 031910.

Montgomery, J.M., Madison, D.V., 2004. Discrete synaptic states define a major mechanism of synapse plasticity. Trends Neurosci. 27 (12), 744–750.

Nakamura, H., O'Leary, D.D., 1989. Inaccuracies in initial growth and arborization of chick retinotectal axons followed by course corrections and axon remodeling to develop topographic order. J. Neurosci. 9 (11), 3776–95.

Perkel, D.H., Gerstein, G.L., Moore, G.P., 1967. Neuronal spike trains and stochastic point processes. Part II. Simultaneous spike trains. Biophys. J. 7, 419–440.

Rakic, P., 1981. Development of visual centers in the primate brain depends on binocular competition before birth. Science 214 4523, 928–931.

Roberts, P.D., Bell, C.C., 2002. Spike timing dependent synaptic plasticity in biological systems. Biol. Cybern. 87, 392–403.

Tetko, I.V., Villa, A.E., 1997. Fast combinatorial methods to estimate the probability of complex temporal patterns of spikes. Biol. Cybern. 76, 397–407.

Tetko, I.V., Villa, A.E., 2001. A pattern grouping algorithm for analysis of spatiotemporal patterns in neuronal spike trains. Part 1. Detection of repeated patterns. J. Neurosci. Meth. 105, 1–14.

Torres, O., Eriksson, J., Moreno, J.M., Villa, A.E., 2004. Hardware optimization and serial implementation of a novel spiking neuron model for the POEtic tissue. BioSystems 76 (1), 201–208.

Tyrrell, A.M., Sanchez, E., Floreano, D., Tempesti, G., Mange, D., 2003. POEtic: an integrated architecture for bio-inspired hardware. Lect. Notes Comput. Sci. 2606, 129–140.

Villa, A.E.P., 2000. Empirical evidence about temporal structure in multi-unit recordings. In: Miller, R. (Ed.), Time and the Brain. Chapter 1. Harwood Academic Publishers, pp. 1–51.